Chinese Chemical Letters 34 (2023) 108165

Contents lists available at ScienceDirect

Chinese Chemical Letters

journal homepage: www.elsevier.com/locate/cclet

Emerging advances in plasmonic nanoassemblies for biosensing and cell imaging

Jin Wang[a,b], Chen Wang[a,b,*], Jing-Juan Xu[b,*], Xing-Hua Xia[b,*], Hong-Yuan Chen[b]

[a] College of Chemistry and Materials Science, Nanjing Normal University, Nanjing 210023, China
[b] State Key Laboratory of Analytical Chemistry for Life Science, School of Chemistry and Chemical Engineering, Nanjing University, Nanjing 210023, China

ARTICLE INFO

Article history:
Received 17 November 2022
Revised 13 January 2023
Accepted 27 January 2023
Available online 31 January 2023

Keywords:
Plasmonic nanoasssembly
Dark-field imaging
Plasmonic circular dichroism
Surface-enhanced Raman scattering
Biosensing
Cell imaging

ABSTRACT

Integrating discrete plasmonic nanoparticles into assemblies can induce plasmonic coupling that produces collective plasmonic properties, which are not available for single nanoparticles. Theoretical analysis revealed that plasmonic coupling derived from assemblies could produce stronger electromagnetic field enhancement effects. Thus, plasmonic assemblies enable better performance in plasmon-based applications, such as enhanced fluorescence and Raman effects. This makes them hold great potential for trace analyte detection and nanomedicine. Herein, we focus on the recent advances in various plasmonic nanoassembles such as dimers, tetramers, and core-satellite structures, and discuss their applications in biosensing and cell imaging. The fabrication strategies for self-assembled plasmonic nanostructures are described, including top-down strategies, self-assembly methods linked by DNA, ligand, polymer, amino acid, or proteins, and chemical overgrowth methods. Thereafter, their applications in biosensor and cell imaging based on dark-field imaging, surface-enhanced Raman scattering, plasmonic circular dichroism, and fluorescence imaging are discussed. Finally, the remaining challenges and prospects are elucidated.

1. Introduction

Plasmonic nanomaterials (Au, Ag, *etc.*) manifest excellent electro-optical properties unrivaled to many conventional materials owing to their unique localized surface plasmon resonance (LSPR) properties, which have demonstrated a wide range of applications in the fields of materials science [1], catalysis [2,3] and life science [4,5], *etc.* [6]. LSPR is defined as when the frequency of incident light coincides with the oscillation frequency of surface plasmons, the free electrons oscillate collectively, while strong resonant absorption or scattering peaks appear in the spectrum [7,8]. By localizing the energy of the light field to the metal surface, the intensity of the electromagnetic field around the metal nanoparticles is enhanced [9]. The LSPR-based optical properties of noble metal nanomaterials are closely related to their morphology, size, composition, dielectric environment, and interparticle spacing, thus the modulation of their optical properties can be achieved in a variety of ways [10,11]. Up to now, numerous works and reviews have been reported on the study of the morphological composition and dielectric environment of plasmonic nanoparticles regarding their LSPR properties [12–14]. Beyond these factors, LSPR properties are closely related to the degree of assembly and dispersion of plasmonic nanoparticles as well. As the near-field coupling between adjacent nanoparticles induces quite stronger local fields, the electromagnetic field strength of plasmonic nanoassemblies is enhanced by several orders of magnitude compared to that of single nanoparticles [15,16]. The intensity of the near-field coupling depends on the spacing of neighboring particles in the assembly, the orientation of the nanoparticle arrangement, and the number of nanoparticles in the assembly. By proper modification of the surface or stimulation from the external field, these parameters can be dynamically regulated during the assembly process, thus successfully achieving the regulation of the optical properties of the assemblies and laying the foundation for the practical applications of the assemblies in various fields [17].

As the most important building blocks for assembly, Au nanoparticles (AuNPs) can be aligned, stacked, and linked together by controlling the position, gap distance, and orientation [18]. Recently, much attention has been paid to the structure and optical activity of AuNPs-based assemblies, and a variety of assembly methods have been developed. These assemblies are constructed by templates or modifying AuNPs with suitable linkers [19]. Based

* Corresponding authors.
E-mail addresses: wangchen@njnu.edu.cn (C. Wang), xujj@nju.edu.cn (J.-J. Xu), xhxia@nju.edu.cn (X.-H. Xia).

https://doi.org/10.1016/j.cclet.2023.108165
1001-8417/

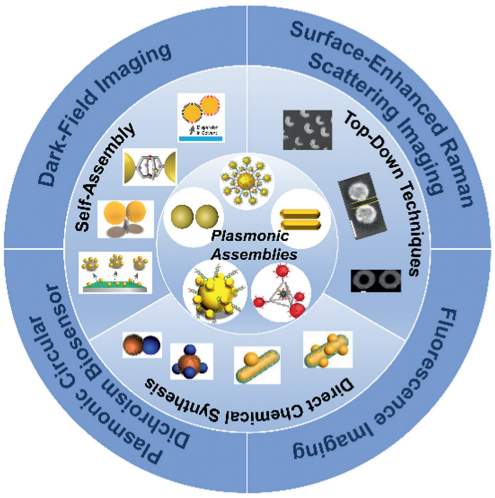

Scheme 1. Schematic illustration of the preparation of plasmonic nanoassemblies and their application in biosensing and cell imaging.

on these methods, numerous nanoassemblies with unique morphology and well-designed structures have been developed, which can be classified as dimer, trimer, multimer, satellite structure, chain, *etc.* according to the aggregation state [15,20]. Among the different assemblies, dimeric nanoparticles consisting of two adjacent nanoparticles are the most basic geometries [21]. Plasmonic dimers possess unique optical activities, for example, red-shifted LSPR in extinction spectra, enhanced electromagnetic fields, and anisotropic optical properties [22]. Multimeric assemblies of trimers and above allow higher-order spatial structures, including two- or three-dimensions [23]. Core-satellite nanostructures are commonly defined as core nanoparticles surrounded by smaller nanoparticles, resulting in a satellite-type layer, a geometry endowing these nanostructures with super-strong coupling properties [24]. Additionally, the construction of one-dimensional chain nanostructures based on templates, molecular linkers, polymers, or ligand-mediated assemblies has also aroused a growing interest [25–27]. Besides the representative nanoassemblies mentioned above, more complex and novel nanostructures have been generated using assembly methods such as DNA origami [28,29].

Plasmonic near-field coupling between neighboring particles in an assembly of noble metal nanoparticles, which yielded a strong localized electromagnetic field, known as a "hot spot", has inspired research related to the preparation of plasmonic nanoassemblies and their application in biosensing and cell imaging [30]. In this review, we aim to summarize recent advances in the construction of Au nanoassemblies with various shapes and functions (Scheme 1). We begin with a brief description of the geometric distinctions of nanoassemblies including dimeric, tetrameric and multimeric with higher orders, core-satellite structures, and nanochains. After that, various fabrication strategies for plasmonic nano-assembled structures are described specifically according to the preparation strategies, including the top-town techniques, self-assembly, and chemical overgrowth methods. The tunability of the optical properties of the assembled plasmonic nanomaterials makes them outstanding nanoplatforms for various biological applications. The following advances in cell analysis- and imaging-related applications will be discussed: (i) dark-field imaging, (ii) surface-enhanced Raman scattering (SERS) imaging, (iii) plasmonic chirality biosensor, and (iv) fluorescence imaging. Finally, the remaining challenges, future developments, and opportunities will be illuminated.

2. Strategies for the preparation of plasmonic nanoassemblies

Since the metal nanoassemblies exhibit excellent properties in many aspects, especially the change of optical properties induced by surface plasmon resonance coupling, their in-depth study has attracted increasing attention. As mentioned earlier, the inter-particle plasmon resonance coupling effect of metal nanoassemblies is closely related to particle morphology, components, and size [9]. In recent years, with the continuous improvement of nanoparticle synthesis and modification techniques, various methodologies for constructing assemblies have been developed. The existing methods can be divided into three major categories, that is, top-down techniques, nanoparticle self-assembly, and chemical synthetic approaches.

2.1. Top-down techniques

The top-down approach means that the substrate is actually a blank canvas and external factors are employed to write the pattern. Conventional fabrication methods such as electron beam lithography, glancing angle physical vapor deposition and focused ion beam have been widely used for the fabrication of nanoassemblies, especially for dimers. In 2003, Rechberger *et al.* prepared Au dimer structures with different spacing using electron beam lithography [31]. Since then, this technique has been refined to prepare Au or Ag nanodimers with different morphologies, and functions [32]. For example, Au nanoring structure-based dimer arrays with different spacings have been reported, which revealed the anomalous sensitivity of nanoring to its anisotropic environment, *i.e.*, asymmetry in particle shape and high index of substrate effects (Figs. S1A-C in Supporting information) [33]. However, expensive instrumentations are often required and the preparation of assemblies with complex composition, narrow interparticle spacing, and three-dimensional structure are difficult to achieve, which greatly limits their further application [34,35].

In this regard, to enable easy fabrication of nanostructures with continuously varying geometric parameters on a single substrate, Ogier *et al.* reported a simple and powerful method, evaporation on partially exposed rotating substrates (PERS), based on controlled relative motion between the supporting substrate and partial shutters during material evaporation to generate continuous and precise gradients in nanoscale structural parameters, including vertical thickness, lateral orientation and direction (Fig. 1A) [36]. Based on this, they successfully prepared a series of Au nanostructures with a wide range of optical response variations, including nanodiscs with continuously varying thicknesses, nanodimers with continuously increasing spacing, and split-ring nanoparticles with continuously varying orientations (Figs. 1B and C). Similarly, Paria *et al.* combined the oblique angle deposition (OAD) technique with a standard graphene transfer protocol to prepare an array of two metal nanoparticles precisely separated by a single layer of graphene. Under light irradiation at appropriate wavelengths, the optical near-field at the particle junctions is strongly enhanced, with an increase of an order of magnitude in the Raman signal in the monolayer graphene [37].

2.2. Self-assembly methods

Self-assembly of nanoparticles mainly involves the modification of functional molecules on the surface of nanoparticles, followed by assembly induced by electrostatic interactions between oppositely charged nanoparticles or coordination chemistry, polymeric linkers, dithiol linkers, proteins, and DNA have been reported [38].

DNA, a versatile and powerful ligand with programmable and sequence-specific interactions, offers great opportunities for assembling nanomaterials. DNA hybridization refers to the formation

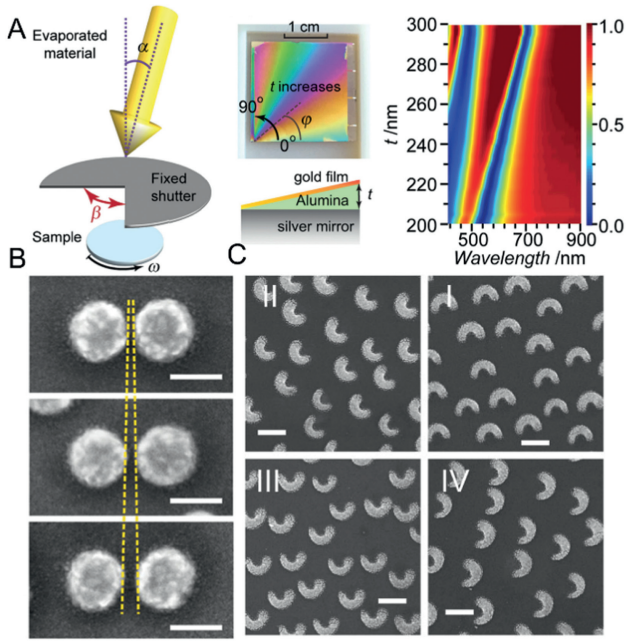

Fig. 1. (A) Fabrication of samples with continuously varying structure parameters. (B) SEM images of representative dimers at $\phi = 0°$, 45°, and 90°, respectively (scale bar = 100 nm). (C) SEM images of split-ring nanostructures taken at the different angular positions (scale bar = 200 nm). Reproduced with permission [36]. Copyright 2016, Wiley-VCH.

of stable structures of DNA molecules linked by hydrogen bonds through the complementary pairing of bases [28]. In 1996, Mirkin *et al.* and Alivisatos *et al.* have demonstrated that DNA could be modified on the surface of AuNPs by Au-S covalent bonding, and further guided by DNA hybridization for Au self-assembly [39,40]. Since then, DNA-mediated AuNPs or other discrete nanoparticles to form continuous one-, two- and three-dimensional structures became one of the main methods for the assembly of nanoparticles [41]. Generally, it is critical to mediate inter-particle interactions for self-assembled DNA nanostructures, which can be achieved by controlling the assembly mode of individual building blocks [28], including direct hybridization [42] and DNA linker-mediated hybridization [43]. While some achievements have been made in the preparation of nanoassemblies based on these DNA hybridization strategies, there are considerable impediments to strong coupling and convenient charge transfer between adjacent nano-units in the assembly. Deng's group developed a chemical tool termed Ag ion soldering (AIS) to overcome the above situation [44]. Briefly, the dimer was first efficiently prepared from AuNPs linked by minimal complementary DNA strands, which were loosely linked by van der Waals (VDW) colloidal interactions, where Ag^+ enhances VDW "gluing" by forming Ag^+-ligand complexes as ligand removers. The immobilized dimers were further modified by fish sperm DNA (FS-DNA) to ensure their colloidal stability in water (Fig. 2A). It is worth mentioning that this method can be successfully used not only for the preparation of Au dimers but also for the fabrication of various heterodimers (such as Au-Pd, Au-Pd, Ag-Pd) with minimal interparticle distances (Fig. S2A in Supporting information) [45]. DNA origami nanostructures are formed by long single-stranded scaffold strands and a suitable set of short artificially short strands [47]. Recently, DNA origami-based template method, where discrete nanoparticles are organized into spatially ordered nanostructures by precisely controlling the interactions between the particles and the DNA template, has also gained extensive attention and exploration over the last few decades [48]. Prompted by the remarkably rich versatility offered by the sequence specificity and spatial addressability of DNA origami templates, DNA origami technology has been exploited by researchers to generate various Au nanoassemblies with unique structural complexity and customizable optical functionality, making them prospective candidates for the construction of innovative Au nanoassemblies. With DNA origami-mediated self-assembly methods, assemblies of gold nanospheres, gold nanorods, gold nanostars, *etc.* with different morphologies have been successfully prepared [49,50]. Tapio *et al.* developed a versatile 3D DNA origami nanofork antenna (DONA) with a gap size as low as 1.17 nm by assembling Au or silver nanoparticle dimers with different gap sizes [46]. Employing oxDNA simulations and atomic force microscopy (AFM), they confirmed that the structure exhibited better overall rigidity over the previous SERS substrate as well as the capability to precisely place biomolecules in the hot spot of the dimer (Fig. 2B). As the development of DNA technology advances, more structurally complex and functionally diverse DNA origami structures will be exploited continuously, which in turn guides the novelty and multifunctionality of nanoassemblies.

Interactions between small molecular ligands immobilized on nanoparticles (*e.g.*, electrostatic interactions, hydrogen bonds, Au-thiol bonds, and molecular cross-linkers) are a common method of self-assembly as well [51–53]. Yoon *et al.* synthesized ideal dimers of Au nanoparticles with smooth surfaces and high sphericity by a substrate-based assembly strategy (Fig. S2B in Supporting information) [54]. By eliminating inhomogeneities caused by variations in gap morphology, unprecedented structural and plasmonic homogeneity was observed at the single-particle level. Due to their orthogonal polarization behavior, contributions from transverse, quadrupole, and octupole longitudinal plasma excitonic coupling modes could be distinguished under the polarization-resolved dark-field scattering spectroscopy. Alternatively, heterodimeric or core-satellite structured assemblies could be prepared by means of chemical linkers for systematic studies of structurally relevant optical properties (Fig. 2C). Due to the close proximity between cores and satellites, strong surface plasmon excitonic coupling was observed from these asymmetric core-satellite nanoassemblies, which appeared to be significantly red-shifted from the LSPR bands. The dependence of the surface plasmon coupling on the gap distance between the core and the satellite was systematically investigated by varying the length of the alkane dithiol linker. As the length of the alkane disulfide linker decreases from 1,16-hexadecanedithiol to 1,2-ethanedithiol, the surface plasmon coupling band is gradually red-shifted, demonstrating enhanced surface plasmon coupling [55].

The excellent processability and flexibility of polymers have been widely recognized and applied in the fields of nanomaterials and biometrics, where polymer-driven self-assembly is also a powerful tool to prepare a wide range of nanoparticle assembly structures [56–58]. To efficiently creation of well-defined dimers with flexible control of structure and further enrich the functionality of plasmonic assemblies for applications in biosensing and nanophotonics, Tian *et al.* proposed a strategy to construct cage-bridged plasmonic dimers based on polymer-assisted self-assembly methods with molecular cage chemistry. The strategy controlled size, composition, shape, symmetry, and interparticle distance in a modular and cost-effective manner with a high degree of freedom and controllability, allowing the easy preparation of various symmetric/asymmetric dimers with gap distances below 5 nm and tailored optical properties (Fig. 2D) [59]. Importantly, the molecular cage embedded in the junction not only acted as a linker between the two constituent elements but also conferred the assembled dimer with the ability to precisely and reversibly enrich the guest molecule in the hot spot region. Most currently constructed plasmonic assemblies exhibit optical signal enhancement that tends uniformly distributed within a hot spot region, while

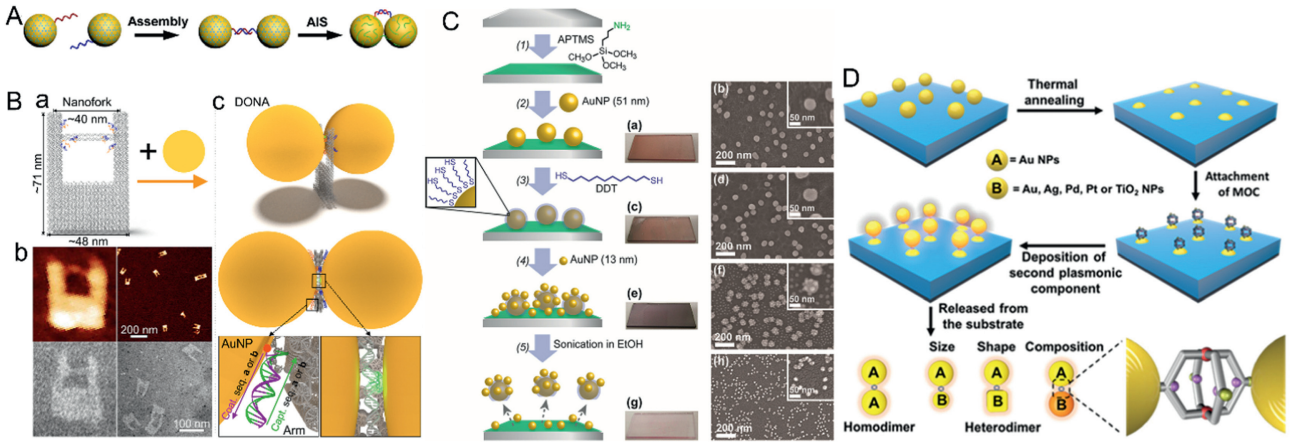

Fig. 2. (A) Schematic illustration of DNA-directed AIS. Reproduced with permission [44]. Copyright 2019, American Chemical Society. (B) Schematic representation of the DNA origami nanofork having a DNA bridge that is 90 nt long (a). AFM and TEM images of the DNA origami nanofork (b). Two differently coated nanoparticles can be attached selectively *via* DNA hybridization to the two different sequences of DNA capture strands on the arms and the bridge of the DNA origami to form DONA structures (c). Reproduced with permission [46]. Copyright 2021, American Chemical Society. (C) The stepwise assembly process for asymmetric core-satellite nanoassemblies using selective desorption. (a-h) Photographic and SEM images of the substrates after each step. Reproduced with permission [55]. Copyright 2021, American Chemical Society. (D) Schematic illustration of the strategy for construction of molecular cage-bridged plasmonic dimer structures. Reproduced with permission [59]. Copyright 2022, American Chemical Society.

precise tuning of site-specific electromagnetic field enhancement by direct assembly processes has been rarely investigated [60]. To address this issue, Zhu *et al.* prepared a series of Janus core-shell nanogapped Au nanoparticles (JAuNNPs) with different degrees of Au shell coverage. The internal nanogaps between the partial Au shells and cores in JAuNNPs led to an asymmetric optical behavior, which can be regulated by changing the internal nanogap [61]. Then a novel type of dimeric nanostructures (core-to-core or shell-to-shell JAuNNDs, Fig. S2C in Supporting information) was prepared by assembling amphiphilic JAuNNPs (50%) coated by different hydrophilic polymers on Au cores and Au shells. Due to the spatial arrangement-related hybrid plasmonic coupling mode, the electromagnetic field enhancement positions of JAuNNPs vary with the geometric configuration.

Amino acids are rich in functional groups, such as amino groups, carboxyl groups, thiols, which can be utilized for the assembly of AuNPs in various ways [62]. Additionally, the introduction of chiral amino acids equipped plasmonic probes with great potential for application. For example, Cys is a special amino acid containing thiols that play a very important role in physiological processes. Since thiol groups can form Au-thiol bonds with AuNPs, the use of Cys-as a linker to AuNPs opens up new avenues for the assembly of AuNPs and has been successfully used for the construction of Au nanorod dimer and multimers of different orientations, with an in-depth investigation of their optical properties [63]. As an emerging functional candidate performing a critical role in specific molecular interactions, peptide is one of the most fundamental biomolecules linking chemistry and biology, affecting important physiological functions [64]. Peptides can be rationally designed and directly immobilized on the surface of AuNPs *via* terminal Cys, for which the peptide-based assembly strategy is similar to that of amino acids, while being equipped with more functionality through carefully designed amino acid sequences [65]. Another assembly strategy is using peptides as templates. Through inorganic recognition motifs, peptides can be specifically recognized and adsorbed on the specific interfaces of AuNPs, as a way to precisely control the location and spatial distribution of AuNPs [66]. Moreover, based on the specific recognition ability of protein molecules, fabrication protocols for nanoassemblies have also been developed. Among them, antigen-antibody-mediated nanoparticle assembly is a widely investigated approach. Based on this strategy, the self-assembly of AuNPs, AuNRs, *etc.* can be achieved and used for the ultra-sensitive detection of some biomolecules [67]. Compared with antigen antibodies, biotin possesses the advantages of small size and high binding capacity. Biotin-avidin system (BAS) is a typical biomagnification system, which is also widely used as a bridge linkage to prepare a variety of directionally assembled nanostructures [68].

Collectively, self-assembly-based methods are more flexible and efficient, though the efficiency and yields of preparation tend to be lower and much exploration in controlled assembly is still needed.

2.3. Chemical synthetic approaches

Recently, a wide range of synthetic protocols have been developed for the synthesis of dimeric and core-satellite structures with controlled composition and properties, such as seed-mediated method [22,69]. Generally, seed-mediated growth consists of two main steps: (i) synthesis of seeds with well-defined structures; (ii) nucleation and growth of the same or another metal on the seed from one or several specific sites [70]. The key to the formation of plasmonic nanoassemblies can be achieved by precise control of several experimental parameters, including the kinetics of reduction, the type of capping agent, and the degree of lattice mismatch between the seeds and the deposited metal [23,71].

The embedding of surface ligands can significantly affect the metal-metal interfacial energy, making it possible to create nanostructures that differ from conventional perceptions [72–74]. Due to the lattice matching of AuNPs and AgNPs, the deposition of Ag on the surface of AuNPs normally results in the formation of concentric core-shell structures. Feng *et al.* managed to prepare Au-Ag Janus structures by surface ligand modification and implemented a continuous regulation from core-shell, eccentric core-shell to dimeric structures by precise regulation of ligands (Fig. S3A in Supporting information). Further studies showed that the surface ligand density and the reduction rate of silver during the synthesis process also have a decisive effect on the nucleation of Ag. A series of Au-Ag satellite nanostructures with different valence of Ag islands were prepared. Eventually, they proposed a depletion sphere mechanism to explain the selection of nucleation sites due to non-stationary concentration gradients. Some other small molecules (*e.g.*, aromatic molecules), as well as biological macromolecules (*e.g.*, DNA), also confirmed the ability to mediate the synthesis of nanoassemblies [75]. Further exploration of plas-

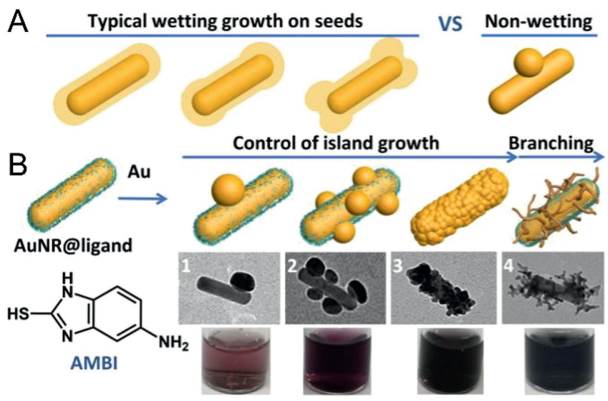

Fig. 3. Schematics illustrating (A) the typical wetting and (B) non-wetting Auon-AuNR homometallic nanostructures, with the corresponding TEM images and photographs. Reproduced with permission [77]. Copyright 2020, Wiley-VCH.

monic nanomaterials is currently devoted to the controlled synthesis of more complex assembly structures, in addition to the design of higher-order nanoassemblies [76]. Jia *et al.* reported a non-wetting growth method that provides two new dimensions of synthetic control in Au-Au homogeneous nanostructures, including the number as well as the shapes of Au islands (Fig. 3A). By controlling the interfacial energy and growth kinetics, they successfully prepared a series of Au-on-Au hybrid nanostructures. The newly grown Au structures could be both spherical and dendritic wires (Fig. 3B). This structural diversity allows the LSPR to be fine-tuned over the full spectral range, making them excellent candidates for plasma applications [77]. Noteworthy, despite the simplicity of this method, its application is limited and it is difficult to achieve the synthesis of complex assembled structures.

3. Application of plasmonic nanoassemblies in biosensing and cell imaging

With the refined design and assembly, plasmonic nanoassemblies possess a variety of physical, chemical, and biological properties that are superior to those of monomeric particles, including unique optical signals, catalytic properties, and local temperature-tuned photothermal properties, *etc.* [78]. In this section, we will focus on reviewing their recent advances in biosensing and bioimaging based on dark-field imaging, SERS imaging, plasmonic circular dichroism-based bioassays and fluorescence-based bioimaging.

3.1. Dark-field microscope (DFM)-based cell imaging

As known, when excited, plasmonic nanoparticles exhibit collective resonant behavior of their surface electrons, and the resonant electrons radiate a light scattering signal with the same oscillation frequency as the exciting light [7]. DFM is a typical optical instrument that can collect and monitor the scattering signal from plasmonic nanoprobes [79]. The assembly process of nanoparticles commonly accompanies the electromagnetic field coupling behavior between the particles, and the enhanced electromagnetic field caused by the coupling is manifested by a significant increase in the scattering intensity and a shift in the scattering wavelength [80]. More importantly, the scattering signal of an individual nanoparticle owns a high sensitivity to the spacing of the assemblies and the degree of coupling. Accordingly, plasmonic nanoassemblies are considered as excellent candidates for dark-field imaging. By monitoring the assembly process and tracking the assemblies in real-time, dynamic and precise analysis of a variety of biomolecules, such as metal ions, enzymes, and miRNA, within cells can be achieved [81,82]. Jun *et al.* designed a core-satellite structured Au nanoassembly as a plasmonic ruler for the study of early caspase-3 activation, achieving long-term monitoring of caspase-3 activity in living cells [83]. As a further extension of this method, Li *et al.* achieved quantitative assessment of miRNA-21 concentrations *in vitro* and *in vivo* utilizing statistical analysis of the time frame over which a strand substitution event occurs *via* DNA-assembled Au core-satellite assemblies (Fig. 4A). The structural and optical stability of the plasmonic probes make it possible to observe continuously for hours without blinking and bleaching under DFM. The combination of dynamic imaging with single-molecule sensitivity and real-time statistical analysis in living cells allows a limited number of nanoprobes to provide accurate quantitative results, fulfilling the practical need to analyze trace amounts of components in single living cells [84,85].

Additionally, relying on their good photostability, excellent sensitivity to environmental media, and optical anisotropy derived from the assembly, plasmonic nanoassemblies can be used in protein-protein interaction studies to capture important nanoscale information, such as protein dimerization as well as their conformational changes through fluctuations in optical signals generated by perturbations. Park *et al.* synthesized monovalent Au (mAu), Au dimers assembled with a Y-shaped oligonucleotide structure (mGYRO) as a rotational probe for monitoring the rotational motion of the membrane protein epidermal growth factor receptor (EGFR) [86]. The conformational changes of the intracellular structural domain of EGFR were revealed at the single-molecule level by monitoring the scattering intensity, successfully decoding the structural dynamics undiscovered in living cells (Fig. 4B).

Moreover, by adjusting the LSPR properties, such as the size, shape and composition of the plasmonic nanoparticles, it is possible to analyze multiple biomolecules simultaneously using DFM techniques. Fan and co-workers previously reported the one-pot synthesis of Au nanostructures with different scattering colors, which were used as labels for real-time quantitative receptor-mediated cytocytosis and intracellular transport of multiple protein-nanoparticle structures in single cells imaging [79]. Alternatively, simultaneous imaging of multiple targets can be achieved based on nanoassemblies by combining different DNA-encoding plasmonic nanoparticles with distinct color distinctions [87]. Nam's group reported a strategy for multiple molecule detection using optokinetically (OK)-encoded nanoprobes (Fig. S4 in Supporting information). Plasmonic nanoparticles with three different dark-field light scattering signals [red (R), green (G) and blue (B)] and partially complementary to three different targets miRNA with mobile (M) or stationary (I) states were attached to a supported lipid bilayer (SLB), respectively. *In situ* single particle monitoring and normalized RGB analysis of the optokinetically combinatorial assemblies among the three M-NPs and the three I-NPs using DFM enabled the differentiation and quantification of nine different miRNA targets in one sample. This multiplex assay enabled the simultaneous detection of multiple miRNA targets in a highly quantitative and specific manner within 1 h and was expected to be used for the diagnosis of different cancer types [88].

3.2. SERS-based cell imaging

SERS is defined as a technique that magnifies the Raman signal from molecules close to the plasmonic substrate with the enhancement of electromagnetic fields from rough metal surfaces. SERS-based detection methods typically feature high sensitivity and spectral resolution, allowing the detection of biological samples in a multiplexed, low background signal and non-invasive manner [89]. Either individual plasmonic nanomaterials or their assembled aggregates are considered to be excellent SERS substrates in terms of electromagnetic field enhancement [15]. How-

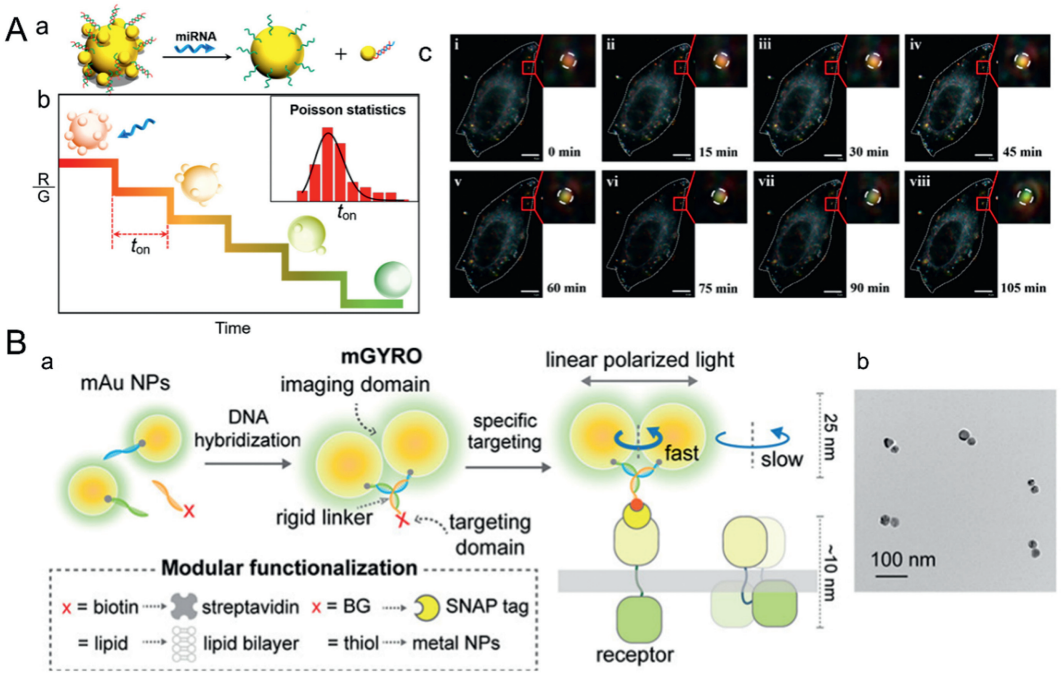

Fig. 4. (A) Structure changes of the PRs induced by miRNA (a), detection principle (b) and continuously imaging of single living HeLa cell after the introduction of PRs (c), scale bar: 10 μm. Reproduced with permission [84]. Copyright 2018, American Chemical Society. (B) Synthesis of mGYROs, conjugating two monofunctionalized Au nanoparticles (mAu NPs) (a), TEM image of mGYRO showing controlled locus of functionalization (b). Reproduced with permission [86]. Copyright 2018, American Chemical Society.

ever, due to the hot spot formation, the plasmonic nanoassemblies often offer stronger Raman enhancement than single nanoparticles and hold considerable potential for applications of SERS-based detection and imaging. With the ultra-strong electromagnetic field in the gap, many nano-assembly-based SERS nanoprobes, including dimer, core-satellite, *etc.*, have been developed for imaging biomolecules such as ATP, miRNA, and enzymes in cells [90–92]. Zhu *et al.* developed a promoted "click" SERS strategy for the highly selective and uniform detection of biomolecules by simultaneous double-enhanced SERS emission (Fig. S5A in Supporting information). Two different triple bond-labeled AuNPs were linked together by DNA hybridization to form a SERS "hot spot" that enabled simultaneous amplification of the triple bonded Raman signal. Specifically, poly A-containing single-stranded DNA and Asp-Glu-Val-Asp (DEVD)-containing peptide sequences were modified onto the alkyne- or nitrile-encoded AuNPs. During apoptosis, the generated caspase-3 would induce cleavage of the tetrapeptide sequence DEVD, which removed the masking of the peptide to the triple bond on AuNPs and the SERS signal was restored (Fig. S5B in Supporting information). This probe realized precise intracellular imaging of caspase-3 in living cells and *in-situ* monitoring of the cell apoptosis process [93].

Considering the ultra-low concentration of intracellular active substances and the limited sensitivity of SESR-based detection, it is urgent to develop engineered nanoparticle assemblies with ultra-strong electromagnetic field [94–96]. Moreover, the off-to-on signal response with higher sensitivity and larger response range facilitates the sensitive detection of intracellular trace substances [97]. Liu *et al.* designed a miRNA-triggered catalytic hairpin assembly-induced core-satellite nanostructure with multiple strong hot spots. This unique plasmonic nanostructure was composed of Au nanodumbbells as the cores, which possessed stronger electromagnetic fields than the common Au nanospheres and Au nanorods (Fig. 5A). The self-assembly strategy triggered by mRNA within the cell could generate SERS signals from off to on, leading to a broad linear detection range of miRNAs from 10^{-19} mol/L to 10^{-9} mol/L. The results of intracellular SERS imaging demonstrated significantly different miRNA expression levels in different cell lines (Figs. 5B and C). The proposed SERS platform facilitated the design of metal nanoparticle assemblies with strong electromagnetic field intensity [98].

3.3. Plasmonic circular dichroism (CD)-based biosensing

The optical chiral signal represents one of the outstanding properties of assembled nanomaterial. Chiral plasmon nanoassemblies are mainly constructed by assembling chiral/achiral plasmonic nanoparticles under the guidance of various chiral molecules/templates [99]. Some chiral molecules, such as amino acids, chiral polymer molecules, DNA/RNA, and peptides, are usually attached to the surface of nanoparticles as chiral linkages or as chiral driving molecules [100]. Experimentally and theoretically have demonstrated that the assembly of asymmetric Au nanostructures (such as dimers, pyramids, and helices) based on chiral molecules, especially DNA and DNA origami, can fine-tune the chiral activity by precisely regulating the assembly process [101,102]. Since the highly dependence of optical activity on the assembled structure, a small structural change may lead to a large change in the chiral signal, thus providing the foundation for the biosensing platform based on chiral plasmonic nanoassemblies [103]. Accordingly, with the optimization and in-depth study of chiral plasmonic nanostructures with CD bands in the visible and near-infrared regions, plasmonic chiral signals have been applied to the hypersensitive analysis of cells [104]. For example, through target-specific chirality or dechirality interactions, changes in CD signal can be established with target concentration changes, providing a zero-background biosensing approach. Such plasmonic chiral sensors have been used to the ultrasensitive detection of metal ions, small molecules, biomolecules in cells [105].

In this regard, Xu's group has successfully prepared a series of plasmonic chiral nanoprobes for cell analysis. To achieve background-free detection of intracellular Zn^{2+}, they constructed

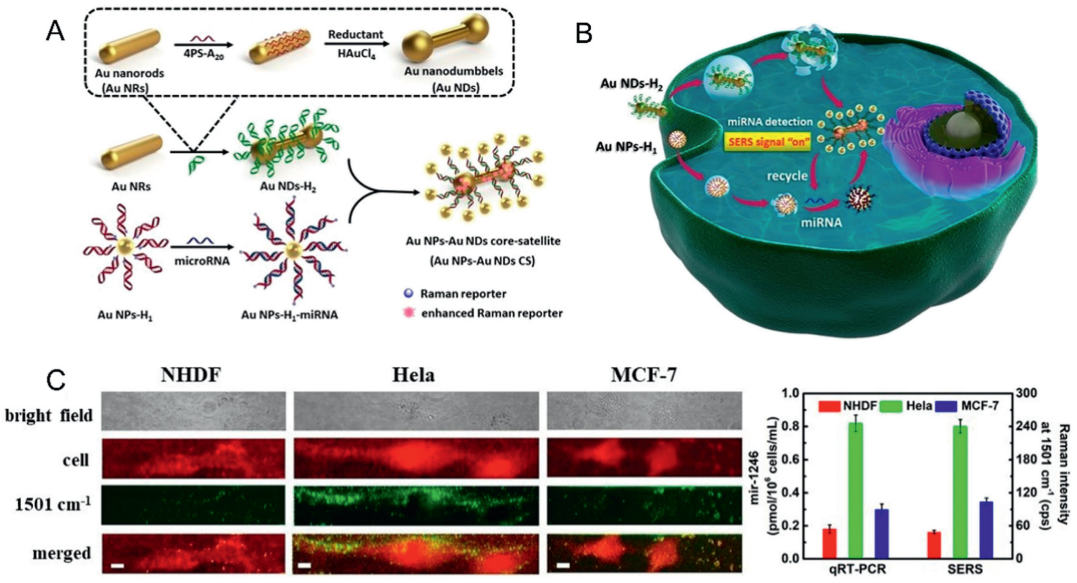

Fig. 5. Schematic Representation of (A) the Fabrication routes of Au NPs-Au NDs CS and (B) Au NPs-Au NDs Core−satellite SERS sensors for miRNA detection and imaging in living cells. (C) Bright-field image and Raman images of HeLa, NHDF, and MCF-7 cells were treated with the mixture of Au NPs-H1 probes and Au NDs-H2 probes, respectively, and the expression level of mir-1246 in NHDF, HeLa, and MCF-7 cells detected by qRT-PCR (left) and Raman intensity at 1501 cm^{-1} detected by CHA strategy (right). Scale bar: 8 μm. Reproduced with permission [98]. Copyright 2018, American Chemical Society.

Au@AgAu yolk-shell nanorods (YSNRs) with significant plasmonic CD response using chiral d/l-Pen (Fig. S6A in Supporting information). Interestingly, their chiral optical response can be tailored by adjusting the gap size or aspect ratio of Au nanorod. The experimental and theoretical results indicated that the hot spot induced by the internal nanogap could enhance the plasmon-induced circular dichroism signal. Further fabrication of YSNR@AuNPs core-satellite assemblies by using chiral YSNRs as chiral building blocks yielded nanostructures with enhanced plasmonic CD activity (Fig. S6B in Supporting information), which are fully suitable for the quantitative detection of intracellular Zn^{2+}. These high-performing chiral nanoassemblies are promising in the fields of chiral catalysis, ultrasensitive biosensors, and optical devices (Figs. S6C-E in Supporting information) [106].

To compensate for the shortage of plasmonic CD in cell imaging, nanoassemblies with multi-signal response capability have attracted the close attention of researchers. As described earlier, plasmonic nanoassemblies could serve as excellent SERS substrates due to the strong electromagnetic fields generated by the plasmonic coupling. As such, by rational design, chiral plasmonic assemblies can function as emitters of both plasmonic CD and SERS signals. Kuang's group reported a bilayer core-satellite structure with high region-controllability and super-strong electromagnetic fields. With the utilization of three types of single-stranded DNA and controlling the amount of DNA on AuNPs, 30, 5, and 10 nm-AuNPs can be controllably assembled into a bilayer nuclear-satellite structure ($C_{30}S_5S_{10}$ NS), by hybridization of specially designed Y-shaped DNA (Fig. 6A). The chiral structure and the SERS tags encoded in the gaps of the particles ensure that the two-layer core-satellite assemblies display strong and controllable CD and SERS signals. The strong CD and SERS signals generated by this assembly can be utilized to realize highly sensitive *in situ* monitoring of miRNAs in living cells (Figs. 6B and C). This superstructure fabrication strategy provides a new access and technological basis for the fabrication of advanced and controllable self-assembled superstructures [107].

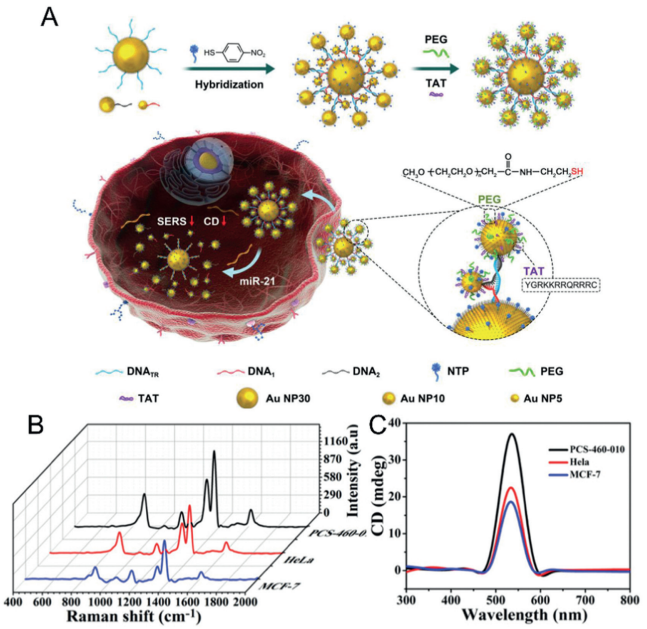

Fig. 6. (A) Schematic representation of Y-DNA-driven construction of Au NP chiral $C_{30}S_5S_{10}$ NSs with enhanced CD and SERS signals. By PEG and TAT modifications, the $C_{30}S_5S_{10}$ NSs was used for ultrasensitive detection of miRNA in living cells. (B, C) SERS spectra (B) and CD spectra (C) of MCF-7, HeLa, and PCS-460–010 cells with $C_{30}S_5S_{10}$ NSs. Reproduced with permission [107]. Copyright 2020, Wiley-VCH.

3.4. Fluorescence-based biosensing and cell imaging

The interaction between fluorescent emission molecules and plasmonic nanoparticles has been extensively studied. On the one hand, Au nanomaterials with high molar extinction coefficients and wide energy bandwidth are an efficient fluorescent quenching agent as a result of the nonradiative interaction between chromophores and metal nanoparticles. Accordingly, researchers have constructed fluorescence resonance energy transfer (FRET) systems by attaching fluorophores to the surface of AuNPs [108]. On the

other hand, the local electric field enhancement induced by plasmon coupling can improve the excitation efficiency and radiation decay rate of chromophores located in the gap region, thus significantly increasing their fluorescence intensity, which is well-known as metal-enhanced fluorescence (MEF) [109]. Assembled metal nanoparticles exhibit better fluorescence enhancement than isolated ones, therefore, nanoassemblies are widely used in MEF-based biosensing systems [110,111]. The influence of different factors such as shape of nanoparticles, dye distribution, and separation distance on fluorescence enhanced by plasmonic coupling was systematically investigated by Zhu *et al.* The fluorescent probe, cyanine 5 (Cy5), was immobilized in the gap region of coupled plasmonic nanoparticles by DNA (Fig. S7A in Supporting information). When Cy5-modified DNA was attached to the surface of AuNPs, the fluorescence of Cy5 was quenched, while the quenched fluorescence of Cy5 was activated after different enhanced substrates, such as Au nanospheres, Au nanorods, Au@Ag core-shell structures, were hybridized with Au-Cy5 to form the nanoassemblies. They found that the formation of assemblies with Au@Ag provided the greatest fluorescence enhancement, and the enhancement factor was stronger with increasing particle size. As the prequenched fluorescence reduced the background of detection, this plasmonic coupling enhanced fluorescence phenomenon was further used to develop a smart fluorescent off-on detection platform for highly sensitive detection of DNA [112]. Furtherly, they investigated the aggregation-induced plasmonic coupled enhancement with single-photon excitation and two-photon excitation using AgNPs, which confirmed that the fluorescence enhancement observed in the coupled nanostructures was mainly attributed to the excitation efficiency of the aggregation-induced plasmonic coupling enhancement [113].

Additionally, many studies have shown that by incorporating inorganic luminescent components (*e.g.*, quantum dots and upconversion nanoparticles, UCNPs) into Au-assembled nanostructures, the signal stability and intensity can be effectively improved compared to organic fluorophores, further facilitating their applications in bioimaging [114]. The AuNR-Pt@Ag_2S, prepared by attaching Ag_2S to Pt-modified AuNRs *via* DNA, was successfully applied for miRNA quantification in the NIR-II region (1000–1700 nm) under 808 nm excitation [115]. A recent work by Kuang and co-workers prepared an UCNPs-centered Au_{20}-Au_{30} nanoparticles tetrahedron (UAuTe) with NIR response by DNA hybridization that selectively accelerated the clearance of senescent cells (Fig. 7). When the beta-2-microglobulin antibody (anti-B2MG) on Au NPs recognized senescent cells, near-infrared light induced the disassembly of UAuTe by splitting the boron ester bond, which released Granzyme B and induces apoptosis of senescent cells. This apoptotic process could be followed by FRET-based signal between UCNP and Cy5 [116].

Notably, apart from the biosensing techniques discussed above, plasmonic nanoassemblies have also been widely used in the fields of photothermal imaging [117,118] as well as electrochemical sensing [119,120] in recent years, mainly attributed to their enhanced electromagnetic fields and ingenious structures that enable great optimization of signals. Research in related fields is also currently in full swing.

4. Conclusion and outlooks

Over the past few decades, advanced optical techniques based on the utilization of plasmonic nanoassemblies as biosensing and imaging probes have developed rapidly. In this review, we focus on the current commonly used types of plasmonic nanoassemblies, including dimers, trimers and higher order multimers, core-satellite structures as well as linear and helical structures, and describe their preparation methods specifically. In addition to the traditional

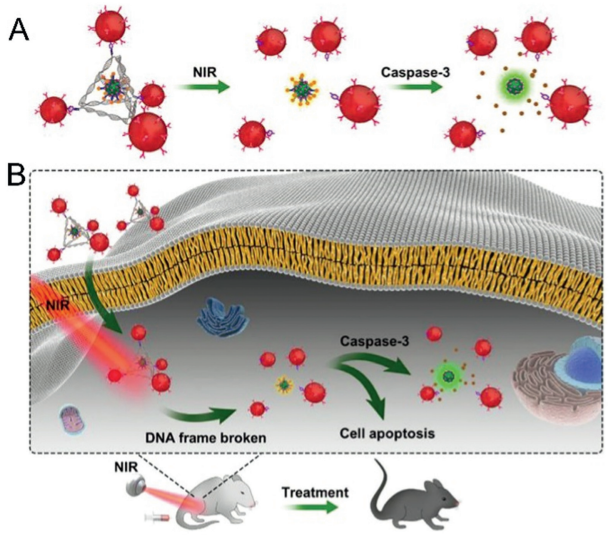

Fig. 7. (A) An NIR-induced dissassembly of UAuTe tetrahedron. (B) The NIR-induced UAuTe tetrahedron used for senescence clearance and apoptosis tracking *in vivo*. Reproduced with permission [116]. Copyright 2020, Wiley-VCH.

top-down methods, current self-assembly methods based on small molecules, polymers, DNA and proteins, as well as the direct chemical synthesis methods, have also received extensive attention and investigations. Generally, these plasmonic nanoassemblies possess many advantages over individual AuNPs, such as stronger electromagnetic fields, more functionality, more flexible responsiveness, and wider applications. Finally, we summarize the recent progress of these plasmonic assemblies based on dark field imaging and single particle scattering spectroscopy, SERS imaging, plasmonic CD, and fluorescence imaging for biosensing and cell imaging applications.

Despite the great progress in the synthesis and optimization of plasmonic nanoassembly structures, many challenges and limitations still exist. First, how to ensure the stability of AuNPs during modification and assembly is a key issue, as the aggregation and decomposition of AuNPs compromise the yield and function of the assemblies, which often require specific surface modifications under precisely controlled experimental conditions. Second, the stability of the assembled structures, high throughput and massive production are concerns that need to be considered and urgently addressed. There is still a need to develop new high-yield methods for the synthesis of monomeric AuNPs and chiral substrate molecules, as well as for the construction of plasmonic nanoassembly structures. Third, the vast majority of currently prepared assemblies are synthesized irreversible, which hinders their flexibility and application range as imaging and diagnostic nanoprobes. Fourth, despite the increasing interest in plasmonic nanoassembly probes in recent decades, their clinical applications are still hampered by many unanswered questions regarding the biological toxicity, structural stability, and biodegradability of the nanoassemblies.

In the future, the construction and application of plasmonic nanoprobes will move on to a new stage of development. Specifically, it can be divided into the following aspects: (1) Exploring novel assembly methods to achieve controlled and reversible construction of nanostructure assembly and disassembly processes will be important for the design of flexible biosensing, cell imaging as well as diagnosis systems. (2) Plasmonic nanomaterials can incorporate more novel elements in the assembly process, which is conducive to the construction of multifunctional plasmonic nanoprobes that can be utilized in the pursuit of more ac-

curate diagnosis and enhanced therapeutic effects. (3) Since the superstructure of plasmonic assemblies can generate stronger electromagnetic fields, the absorption and emission of light in the NIR-II region can be achieved through reasonable structural tuning and optimization, which is certainly a good candidate for future diagnostic and therapeutic applications. (4) In terms of plasmonic CD, the development of tunable and high yield chiral nanostructure assembly methodology, combined with the ongoing improvement of the sensitivity and reliability of chiral-based biosensors, will significantly benefit their development in the field of biosensing and disease diagnosis.

Declaration of competing interest

The authors declare that they have no known competing financial interests or personal relationships that could have appeared to influence the work reported in this paper.

Acknowledgments

This work was supported by grants from the National Natural Science Foundation of China (Nos. 22022412, 22274076, 21874155), the Primary Research & Development Plan of Jiangsu Province (No. BE2022793).

Supplementary materials

Supplementary material associated with this article can be found, in the online version, at doi:10.1016/j.cclet.2023.108165.

References

[1] M. Sharifi, F. Attar, A.A. Saboury, et al., J. Control. Release 311-312 (2019) 170–189.
[2] J. Li, Z. Lou, B. Li, Chin. Chem. Lett. 33 (2022) 1154–1168.
[3] D. Liu, N. Yang, Q. Zeng, et al., Chin. Chem. Lett. 32 (2021) 3288–3297.
[4] Y. Zhao, X.Y. Gao, H. Wang, et al., Anal. Chem. 91 (2019) 15988–15992.
[5] Y. Wu, M.R.K. Ali, K. Chen, N. Fang, M.A. El-Sayed, Nano Today 24 (2019) 120–140.
[6] S.S. Wang, X.P. Zhao, F.F. Liu, et al., Anal. Chem. 91 (2019) 4413–4420.
[7] K.M. Mayer, J.H. Hafner, Chem. Rev. 111 (2011) 3828–3857.
[8] M. Rycenga, C.M. Cobley, J. Zeng, et al., Chem. Rev. 111 (2011) 3669–3712.
[9] S. Lee, Y. Sun, Y. Cao, S.H. Kang, Trends Analyt. Chem. 117 (2019) 58–68.
[10] P.F. Gao, Y.F. Li, C.Z. Huang, Appl. Spectrosc. Rev. 54 (2019) 237–249.
[11] X.W. Liao, Q.Y. Xu, Z. Tan, Y. Liu, C. Wang, Electroanal. 34 (2021) 923–936.
[12] L. Zhu, Z. Lu, L. Zhang, N. He, Chin. Chem. Lett. 33 (2022) 2491–2495.
[13] B. Zhang, Y. Xia, Chin. Chem. Lett. 30 (2019) 1663–1666.
[14] A. Liu, M. Li, J. Wang, et al., Chin. Chem. Lett. 31 (2020) 1133–1136.
[15] S. Lee, K. Sim, S.Y. Moon, et al., Adv. Mater. 33 (2021) e2007668.
[16] R.E. Armstrong, M. Horacek, P. Zijlstra, Small 16 (2020) e2003934.
[17] P. Dey, T.A. Tabish, S. Mosca, et al., Small 16 (2020) e1906780.
[18] M.Q. He, Y.L. Yu, J.H. Wang, Nano Today 35 (2020) 101005.
[19] Q. Fu, Z. Li, F. Fu, et al., Nano Today 36 (2021) 101014.
[20] R. Zhu, J. Li, L. Lin, J. Song, H. Yang, Adv. Funct. Mater. 31 (2020) 2005709.
[21] A.R. Salmon, M.E. Kleemann, J. Huang, et al., ACS Nano 14 (2020) 4982–4987.
[22] Z. Wu, L. Li, T. Liao, et al., Nano Today 22 (2018) 62–82.
[23] M. Ha, J.H. Kim, M. You, et al., Chem. Rev. 119 (2019) 12208–12278.
[24] N. Pazos-Perez, J.M. Fitzgerald, V. Giannini, L. Guerrini, R.A. Alvarez-Puebla, Nanoscale Adv. 1 (2019) 122–131.
[25] T. Chen, M. Pourmand, A. Feizpour, B. Cushman, B.M. Reinhard, J. Phys. Chem. Lett. 4 (2013) 2147–2152.
[26] Z. Zhu, W. Liu, Z. Li, et al., ACS Nano 6 (2012) 2326–2332.
[27] M.N. Biutty, M. Zakia, S.I. Yoo, Bull. Korean Chem. Soc. 41 (2020) 1033–1039.
[28] N. Liu, T. Liedl, Chem. Rev. 118 (2018) 3032–3053.
[29] K. Martens, F. Binkowski, L. Nguyen, et al., Nat. Commun. 12 (2021) 2025.
[30] F. Li, J. Lu, X. Kong, T. Hyeon, D. Ling, Adv. Mater. 29 (2017) 1605897.
[31] W. Rechberger, A. Hohenau, A. Leitner, et al., Opt. Commun. 220 (2003) 137–141.
[32] S.S. Acimovic, M.P. Kreuzer, M.U. Gonzalez, R. Quidant, ACS Nano 3 (2009) 1231–1237.
[33] R. Near, C. Tabor, J. Duan, R. Pachter, M. El-Sayed, Nano Lett. 12 (2012) 2158–2164.
[34] O. Colomer-Ferrer, S. Toda Cosi, Y. Conti, et al., J. Mater. Chem. C 10 (2022) 13913–13921.
[35] X. Wu, C. Hao, J. Kumar, et al., Chem. Soc. Rev. 47 (2018) 4677–4696.
[36] R. Ogier, L. Shao, M. Svedendahl, M. Kall, Adv. Mater. 28 (2016) 4658–4664.
[37] D. Paria, K. Roy, H.J. Singh, et al., Adv. Mater. 27 (2015) 1751–1758.
[38] L. Lermusiaux, A. Nisar, A.M. Funston, Nano Res. 14 (2020) 635–645.
[39] C.A. Mirkin, R.L. Letsinger, R.C. Mucic, J.J. Storhoff, Nature 382 (1996) 607–609.
[40] A.P. Alivisatos, K.P. Johnsson, X.G. Peng, et al., Nature 382 (1996) 609–611.
[41] Y. Zhao, C. Xu, Adv. Mater. 32 (2020) e1907880.
[42] X. Lan, Z. Chen, B.J. Liu, et al., Small 9 (2013) 2308–2315.
[43] X.L. Li, Z.L. Zhang, W. Zhao, et al., Chem. Sci. 7 (2016) 3256–3263.
[44] Y. Li, Z. Deng, Acc. Chem. Res. 52 (2019) 3442–3454.
[45] X. Song, Y. Wang, Y. Hao, et al., Chem. Sci. 13 (2022) 4788–4793.
[46] K. Tapio, A. Mostafa, Y. Kanehira, et al., ACS Nano 15 (2021) 7065–7077.
[47] J. Lee, J.H. Huh, K. Kim, S. Lee, Adv. Funct. Mater. 28 (2018) 1707309.
[48] J. Ryssy, A.K. Natarajan, J. Wang, et al., Angew. Chem. Int. Ed. 60 (2021) 5859–5863.
[49] S. Tanwar, K.K. Haldar, T. Sen, J. Am. Chem. Soc. 139 (2017) 17639–17648.
[50] H. Yu, T. Man, W. Ji, et al., Chin. Chem. Lett. 30 (2019) 175–178.
[51] H. Cha, J.H. Yoon, S. Yoon, ACS Nano 8 (2014) 8554–8563.
[52] T. Li, J. Sun, J. Liu, et al., Chin. Chem. Lett. 31 (2020) 439–442.
[53] L.L. Tan, M. Wei, L. Shang, Y.W. Yang, Adv. Funct. Mater. 31 (2020) 2007277.
[54] J.H. Yoon, F. Selbach, L. Langolf, S. Schlucker, Small 14 (2018) 1702754.
[55] J.H. Yoon, J. Lim, S. Yoon, ACS Nano 6 (2012) 7199–7208.
[56] J.F. Stoddart, Nat. Chem. 1 (2009) 14–15.
[57] S. Das, P. Ranjan, P.S. Maiti, et al., Adv. Mater. 25 (2013) 422–426.
[58] S.A.A. Kooijmans, L.A.L. Fliervoet, R. van der Meel, et al., J. Control. Release 224 (2016) 77–85.
[59] L. Tian, C. Wang, H. Zhao, et al., J. Am. Chem. Soc. 143 (2021) 8631–8638.
[60] T. Ding, A.W. Rudrum, L.O. Herrmann, V. Turek, J.J. Baumberg, Nanoscale 8 (2016) 15864–15869.
[61] R. Zhu, H. Feng, Q. Li, et al., Angew. Chem. Int. Ed. 60 (2021) 12560–12568.
[62] M.S. Inkpen, Z.F. Liu, H. Li, et al., Nat. Chem. 11 (2019) 351–358.
[63] B. Han, Z. Zhu, Z. Li, W. Zhang, Z. Tang, J. Am. Chem. Soc. 136 (2014) 16104–16107.
[64] J. Lu, Y.X. Chang, N.N. Zhang, et al., ACS Nano 11 (2017) 3463–3475.
[65] X. Li, Z. Wu, X. Zhou, J. Hu, Biosens. Bioelectron. 92 (2017) 496–501.
[66] A.D. Merg, J.C. Boatz, A. Mandal, et al., J. Am. Chem. Soc. 138 (2016) 13655–13663.
[67] S. Zhu, R. Tian, A.L. Antaris, X. Chen, H. Dai, Adv. Mater. 31 (2019) e1900321.
[68] C.Y. Poon, L. Wei, Y. Xu, et al., Anal. Chem. 88 (2016) 8849–8856.
[69] X. Liang, X. Du, A. Liu, et al., Chin. Chem. Lett. 34 (2023) 107491.
[70] J. Qiu, Q.N. Nguyen, Z. Lyu, Q. Wang, Y. Xia, Adv. Mater. 34 (2022) e2102591.
[71] J. Wang, D. Luo, Y.D. Cai, et al., Biosens. Bioelectron. 213 (2022) 114422.
[72] F. Zheng, W. Ke, L. Shi, H. Liu, Y. Zhao, Anal. Chem. 91 (2019) 11812–11820.
[73] Y. Feng, J. He, H. Wang, et al., J. Am. Chem. Soc. 134 (2012) 2004–2007.
[74] J. Huang, Y. Zhu, C. Liu, et al., Nano Lett. 16 (2016) 617–623.
[75] Y. Feng, Y. Wang, X. Song, S. Xing, H. Chen, Chem. Sci. 8 (2017) 430–436.
[76] Q.K. Fan, K. Liu, J. Feng, et al., Adv. Funct. Mater. 28 (2018) 1803199.
[77] J. Jia, G. Liu, W. Xu, et al., Angew. Chem. Int. Ed. 59 (2020) 14443–14448.
[78] A. Klinkova, R.M. Choueiri, E. Kumacheva, Chem. Soc. Rev. 43 (2014) 3976–3991.
[79] J. Shen, L. Liang, M. Xiao, et al., J. Am. Chem. Soc. 141 (2019) 11938–11946.
[80] Y. Guo, Y. Liu, W. Zhou, G. Wang, ACS Sens. 6 (2021) 958–966.
[81] P.F. Gao, G. Lei, C.Z. Huang, Anal. Chem. 93 (2021) 4707–4726.
[82] T.T. Zhai, D. Ye, Y. Shi, et al., ACS Appl. Mater. Interfaces 10 (2018) 33966–33975.
[83] Y.W. Jun, S. Sheikholeslami, D.R. Hostetter, et al., Proc. Natl. Acad. Sci. U. S. A. 106 (2009) 17735–17740.
[84] M.X. Li, W. Zhao, H. Wang, et al., Anal. Chem. 90 (2018) 14255–14259.
[85] M.X. Li, C.H. Xu, N. Zhang, et al., ACS Nano 12 (2018) 3341–3350.
[86] Y. Park, S. Shin, H. Jin, et al., J. Am. Chem. Soc. 140 (2018) 15161–15165.
[87] S. Kim, J.E. Park, W. Hwang, et al., J. Am. Chem. Soc. 139 (2017) 3558–3566.
[88] Y.K. Lee, S. Kim, J.W. Oh, J.M. Nam, J. Am. Chem. Soc. 136 (2014) 4081–4088.
[89] S. Liu, Y. Ying, Y. Long, Chin. Chem. Lett. 31 (2020) 473–475.
[90] J.M. Kim, C. Lee, Y. Lee, et al., Adv. Mater. 33 (2021) e2006966.
[91] D. Wu, Y. Chen, S. Hou, W. Fang, H. Duan, ChemBioChem 20 (2019) 2432–2441.
[92] X. Zhang, Y. Ge, M. Liu, et al., Anal. Chem. 94 (2022) 7823–7832.
[93] W. Zhu, C.Y. Wang, J.M. Hu, A.G. Shen, Anal. Chem. 93 (2021) 4876–4883.
[94] C. Zong, M. Xu, L.J. Xu, et al., Chem. Rev. 118 (2018) 4946–4980.
[95] Q. Li, X. Ge, J. Ye, et al., Angew. Chem. Int. Ed. 60 (2021) 7323–7332.
[96] C. Dong, X. Fang, J. Xiong, et al., ACS Nano 16 (2022) 14055–14065.
[97] C. Liu, T. Xu, G. Cheng, X. Zhang, Sens. Actuators B: Chem. 330 (2021) 129319.
[98] C. Liu, C. Chen, S. Li, et al., Anal. Chem. 90 (2018) 10591–10599.
[99] Y. Wen, Z. Li, J. Jiang, Chin. Chem. Lett. 30 (2019) 1565–1574.
[100] X.T. Kong, L.V. Besteiro, Z. Wang, A.O. Govorov, Adv. Mater. 32 (2020) e1801790.
[101] B.H. Lee, N.A. Kotov, G. Arya, ACS Nano 15 (2021) 13547–13558.
[102] L. Nguyen, M. Dass, M.F. Ober, et al., ACS Nano 14 (2020) 7454–7461.
[103] W. Ma, L. Xu, L. Wang, C. Xu, H. Kuang, Adv. Funct. Mater. 29 (2019) 1805512.
[104] H. Li, X. Gao, C. Zhang, et al., Biosensors 12 (2022) 957.
[105] L. Xu, Y. Gao, H. Kuang, L.M. Liz-Marzan, C. Xu, Angew. Chem. Int. Ed. 57 (2018) 10544–10548.
[106] C.L. Hao, L.G. Xu, M.Z. Sun, et al., Adv. Funct. Mater. 28 (2018) 1802372.
[107] D. Meng, W. Ma, X. Wu, C. Xu, H. Kuang, Small 16 (2020) e2000003.
[108] X. Shen, W. Xu, J. Ouyang, N. Na, Chin. Chem. Lett. 33 (2022) 4505–4516.
[109] R. Ranjan, E.N. Esimbekova, M.A. Kirillova, V.A. Kratasyuk, Anal. Chim. Acta 971 (2017) 1–13.
[110] M. Garai, N. Gao, Q.H. Xu, J. Phys. Chem. C 122 (2018) 23102–23110.

[111] D. Botequim, I.I.R. Silva, S.G. Serra, et al., Nanoscale 12 (2020) 6334–6345.
[112] Z.J. Zhu, P.Y. Yuan, S. Li, et al., ACS Appl. Bio Mater. 1 (2018) 118–124.
[113] D.F. Zhang, S. Li, Q.H. Xu, Y. Cao, Langmuir 36 (2020) 4721–4727.
[114] R. Gao, L. Xu, C. Hao, C. Xu, H. Kuang, Angew. Chem. Int. Ed. 58 (2019) 3913–3917.
[115] A.H. Qu, L.G. Xu, M.Z. Sun, et al., Adv. Funct. Mater. 27 (2017) 1703408.
[116] A. Qu, X. Wu, S. Li, et al., Adv. Mater. 32 (2020) e2000184.
[117] R.A. Guzman, G.G. Rubio, J.G. Izquierdo, et al., ACS Omega 1 (2016) 388–395.
[118] M. Kim, J.H. Lee, J.M. Nam, Adv. Sci. 6 (2019) 1900471.
[119] Q.Y. Xu, Z. Tan, X.W. Liao, C. Wang, Chin. Chem. Lett. 33 (2022) 22–32.
[120] Q. Zhang, Y. Tian, Z. Liang, et al., Anal. Chem. 93 (2021) 3308–3314.